ELSEVIER

CMIG Extra: Cases 29 (2005) 27–32

Computerized Medical Imaging and Graphics

www.elsevier.com/locate/compmedimag

Case report

Magnetization transfer ratio and apparent diffusion coefficient analysis in children with global developmental delay

Margaret H. Pui *, Yongdong Wang, Nina Singh

Department of Radiology, McMaster University Medical Centre, 1200 Main Street West, Hamilton, Ont., Canada L8N 3Z5

Received 14 January 2005; accepted 3 October 2005

Abstract

Global developmental delay has a significant socioeconomic impact. Early identification of the etiology can obviate further diagnostic testing. Magnetization transfer imaging and diffusion-weighted imaging were performed on 85 children with global developmental delay and 133 normally developed children as control. Conventional MRI was abnormal in all of the 41 children with congenital brain malformation, metabolic and chromosomal disorders, and vitamin B12 deficiency, 85.71% of the seven children with genetic syndrome, and 60% of the five children with history of viral encephalitis. Although magnetization transfer ratios and apparent diffusion coefficients were abnormal in these children, there was no specific pattern to aid the differential diagnosis. Eight of the 13 children with clinical suspicion of cerebral palsy had abnormal MRI findings that may help to reclassify them as having congenital malformation. All of 19 children who were eventually classified as idiopathic global developmental delay had normal MRI. The diagnostic yield of electroencephalogram, metabolic screening, cytogenetic testing, and skin/muscle biopsy was low at 62.50, 24.71, 22.22, and 19.05%, respectively.

Keywords: Magnetic resonance imaging; Magnetization transfer; Diffusion imaging; Global developmental delay

1. Introduction

Global developmental delay (GDD) is defined as significant delay in two or more of the developmental domains including gross or fine motor, speech or language, cognition, social or personal development, and activities of daily living. Prevalence of GDD is 1–3% and has a significant socioeconomic impact [1]. Disorders associated with GDD include metabolic or chromosomal abnormalities, genetic syndromes, and acquired cerebral insults. Detailed history and physical examination can identify the etiology in 17–34% of cases. CT and MRI delineate acquired injury and congenital anomaly of the central nervous system with diagnostic yield of 30 and 66%, respectively [2–6]. Metabolic screening including urine organic acids, arterial blood gases, plasma amino acids, ammonia, and lactate has a diagnostic yield of 42% whereas molecular cytogenetic testing has a low yield of 3.5–10% [4,7–9]. Early identification of the etiology of the GDD can obviate further diagnostic testing.

Conventional MRI uses the T1 and T2 relaxation times and proton density of tissue water to manipulate contrast. Tissues contain both a free hydrogen pool and an immobile hydrogen pool bound to macromolecular proteins and lipids. Direct observation of the immobile hydrogen pool is normally not possible because of its short T2 relaxation time of <200 μs. By applying an off-resonance radiofrequency pulse in magnetization transfer imaging (MTI) to saturate the restricted pool, the signal of the free pool is decreased because of magnetization transfer from the immobile to mobile protons. MTI reflects the structural integrity of the tissue being imaged and has been used as a method of contrast enhancement, background suppression and tissue characterization in magnetic resonance angiography and evaluation of white matter lesions, brain infarct, brain tumors, and neurodegenerative disorders [10–16]. Microscopic behavior of tissues can also be examined by diffusion-weighted imaging (DWI) through the random translational mobility of water molecules. By applying equal and opposite gradients on either side of a refocusing

* Corresponding author. Address: 88 Heddington Avenue, Toronto, Ont., Canada M5N 2K8. Tel.: +1 416 481 3139; fax: +1 416 431 8141.
E-mail address: puimarg@yahoo.ca (M.H. Pui).

1572-3496/$ - see front matter © 2005 Elsevier Ltd. All rights reserved.
doi:10.1016/j.compmedimag.2005.10.003

lobe in a standard pulse sequence, protons in tissue without motion are initially dephased and become rephased by the opposite gradients. Mobile protons are not rephased, thus resulting in decreased signal intensity. The amount of signal loss is a marker of movement of free water and allows indirect evaluation of tissue microstructure. DWI has been used for investigation of brain tumors, ischemia, and infection in children [17–21]. The purpose of this study was to determine the complementary value of magnetization transfer ratio (MTR) and apparent diffusion coefficient (ADC) to conventional MRI and other investigations in identifying the etiology of GDD.

2. Materials and methods

From February 2002 through April 2003, 85 consecutive children (51 boys, 34 girls, age range: newborn to 18 years, average: 4.05 years) who were referred for MRI evaluation of GDD were enrolled in the study. The control group consisted of 85 boys and 48 girls (age range: newborn to 18 years, average: 8.96 years) with normal development who underwent MRI for pre-operative assessment of brain tumors. Informed consent was obtained from their parents and intravenous sedation was used in younger children. MTI and DWI were performed using a head coil on a 1.5 T MR system (Siemens Symphony, Erlangen, Germany). Axial turbo spin-echo T1-weighted (repetition time TR 460 ms/echo time TE 15 ms/90° flip angle/two acquisitions/19 slices/5 mm slice thickness/1 mm inter-slice gap, echo factor 8, 20 cm field of view), T2-weighted (3610/98/90°/2/19/5/1), and coronal fluid-attenuated inversion-recovery (9000/99/90°/1/19/5/1/inversion time TI 2500 ms)-weighted images were acquired. Axial gradient-echo fast low angle shot (FLASH) images were obtained (160/14/15°/1/14/5/1, 176×256 matrix, 1 min 26 s acquisition time, 78 Hz/pixel bandwidth) with and without MTI pulse (gaussian envelope duration 7.68 ms, 500°, 1.5 kHz frequency offset). The MTR analysis using MT-prepared gradient-echo sequence has previously been shown to yield favorable sensitivity and specificity in differentiating brain tumor, infection, and infarction in adults and children [22,23]. Axial DWI was performed using fat-saturated single-shot spin-echo echo planar imaging (EPI) sequence (220/139/90°/4/19/5/1, 128×128, 50 s acquisition time, 1346 Hz/pixel, EPI factor 128, $b=0$, 900 mm^2/s in three orthogonal directions). Regions of interest (ROI) were drawn on the ADC map by one radiologist (MP) on the frontal and parietal cortical gray matter, frontal and parietal deep white matter, head of caudate nucleus, putamen, globus pallidus, thalamus, substantia nigra, tectum, and middle cerebellar peduncle. ADC of cerebrospinal fluid was used as internal control by placing ROI in the ventricles. The T1- and T2-weighted images were used as guide to delineate the anatomical structures for ADC and MTR determination. In the control group, the ROI were drawn in normal brain tissue remote from the tumor. MTR was calculated using the equation: $MTR = 100 \times (SI_0 - SI_m)/SI_0$, where SI_0 and SI_m were the signal intensities of the ROI on the FLASH images without and with MTI pulse, respectively. The children were separated into groups according to gender and 1-year interval from <1 to <18 years of age. The MTRs and ADCs were compared to the age- and sex-matched normal control using the Wilcoxon signed-rank test for paired samples. Statistical significance was defined as $p < .05$. The final diagnosis was obtained based on a combination of history, physical examination, conventional MRI, metabolic screening, molecular cytogenetic analysis, and/or muscle biopsy.

3. Results

Table 1 categorizes the study subjects by age and gender. The number of children with different causes for GDD, EEG, metabolic, MRI, cytogenetic testing, and skin/muscle biopsy abnormality is listed in Table 2. Of the children with GDD who were investigated, 62.50% (25/40) had abnormal EEG, 24.71% (21/85) had metabolic abnormality, 68.24% (58/85) had abnormal findings on conventional MRI, 22.22% (6/27) had abnormal cytogenetic testing, and 19.05% (4/21) had abnormal skin/muscle biopsy.

Brain malformation was detected in 27 children by conventional MRI including microencephaly (13), hydrocephalus (8), lissencephaly (5), posterior fossa cyst (3), delayed myelination or dysmyelination (3), hypogenesis of corpus callosum (2), Chiari malformation (2),

Table 1
Age and gender distribution of the study subjects

Age range	Normal control		Global developmental delay	
Years	Male	Female	Male	Female
<1	12	5	13	2
<2	4	4	5	6
<3	5	2	9	6
<4	4	0	3	0
<5	4	3	7	4
<6	4	2	2	5
<7	4	2	3	2
<8	2	2	2	2
<9	5	3	2	1
<10	5	3	1	3
<11	10	3	1	0
<12	4	3	1	1
<13	5	4	1	0
<14	3	2	1	0
<15	5	4	0	0
<16	4	2	0	1
<17	4	2	0	0
<18	1	2	0	1
Total	85	48	51	34

Table 2
Etiology, EEG, metabolic and MRI abnormality in children with global developmental delay

	Number of children	Abnormal EEG	Metabolic abnormality	MRI abnormality	Cytogenetic abnormality	Abnormal skin/ muscle biopsy
Brain malformation	27	6/10	6/27	27/27	0/4	0/1
Metabolic disorder	6	2/2	6/6	6/6	0/2	1/6
Chromosomal abnormality	6	4/4	0/6	6/6	6/6	0
Genetic syndromes	7	3/3	2/7	6/7	0/1	2/3
Post-viral encephalitis	5	2/4	0/5	3/5	0/1	0
Vitamin B12 deficiency	2	1/2	2/2	2/2	0/1	0
Cerebral palsy	13	3/5	3/13	8/13	0/4	1/7
Idiopathic developmental delay	19	4/10	2/19	0/19	0/8	0/4
Total	85	25/40	21/85	58/85	6/27	4/21

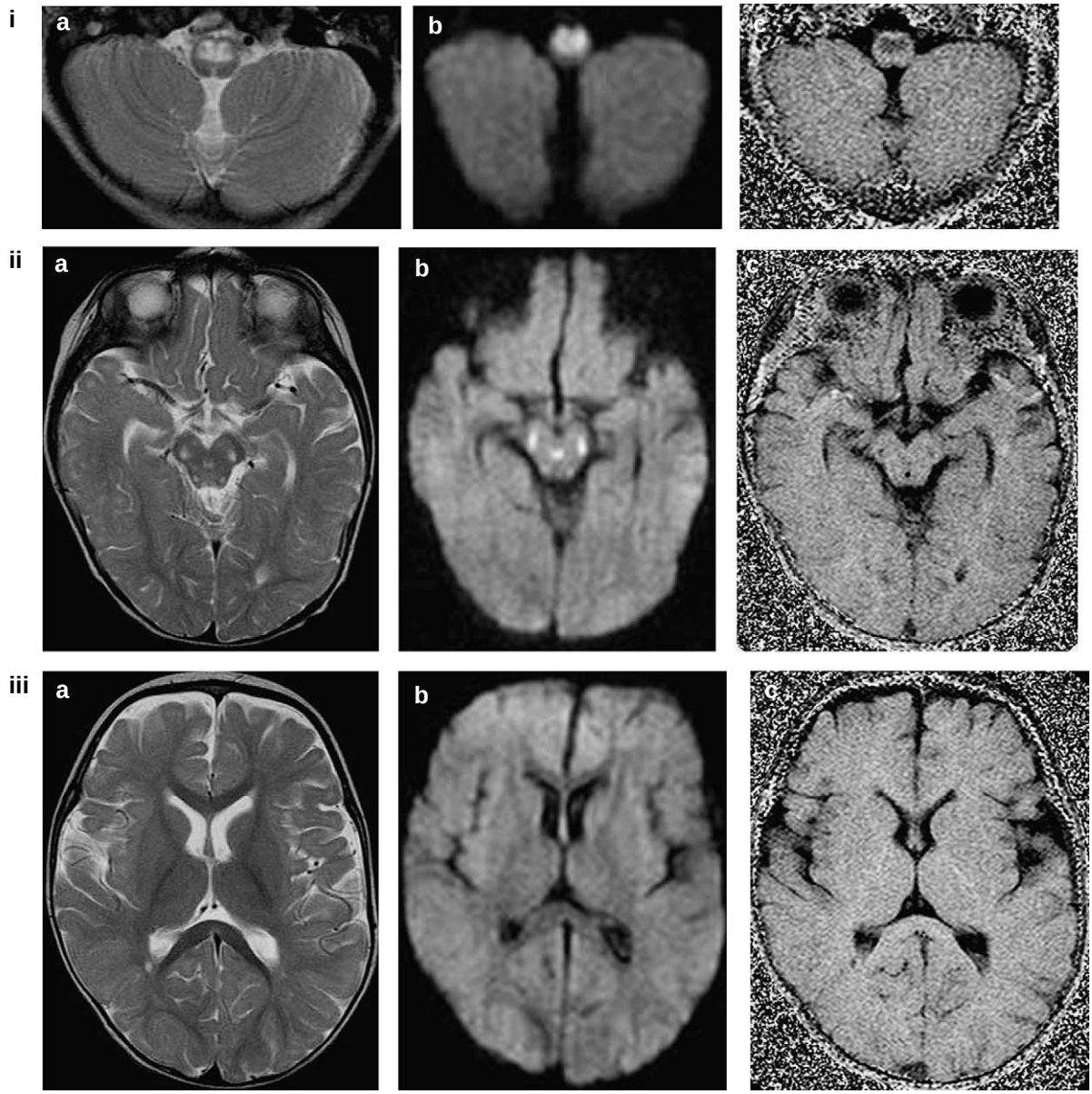

Fig. 1. A 10-month-old boy with Leigh's disease and global developmental delay. (ia) Axial T2-weighted image shows hyperintensity in the medulla-cervical cord anteriorly suggesting dysmyelination. The lesions are hypointense on T1-weighted image (not shown). (ib) Diffusion-weighted image and (ic) MTR map demonstrates MTR as low signal intensity in the corresponding white matter tracts (iia) T2-weighted image at midbrain level in the same child shows symmetrical dysmyelination in bilateral substantia nigra laterally, colliculi, and periaqueductal gray matter. Low ADC and low MTR are demonstrated as high and low signal intensities on the (iib) diffusion-weighted image and (iic) MTR map, respectively. The occipital periventricular white matter lesions in the same patient are more chronic with (iiia) T2 prolongation, (iiib) normal diffusion, and (iiic) slightly low MTR.

holoprosencephaly (1), pituitary hypoplasia (1), and optic nerve hypoplasia (1). The mean MTRs of cortical gray matter ($37.19 \pm 4.34\%$) were significantly ($p = .046$) lower than normal control ($38.81 \pm 1.92\%$). MTRs of thalamus ($42.04 \pm 2.92\%$) were significantly ($p = .026$) higher than normal control ($40.66 \pm 2.44\%$) whereas ADCs of tectum ($1.14 \pm 0.14 \times 10^{-3}$ mm^2/s) were significantly ($p = .028$) lower than normal control ($1.23 \pm 0.11 \times 10^{-3}$ mm^2/s).

Conventional MRI showed T2 prolongation and T1 shortening in the white matter, basal ganglia, and/or brainstem of all six children with metabolic disorders. The ADCs of parietal white matter ($1.35 \pm 0.15 \times 10^{-3}$ mm^2/s) and MTRs of putamen ($41.74 \pm 1.51\%$) were significantly ($p = .046$, .043) higher than normal control ($1.20 \pm 0.21 \times 10^{-3}$ mm^2/s, $39.66 \pm 1.70\%$), whereas ADCs of substantia nigra ($0.97 \pm 0.03 \times 10^{-3}$ mm^2/s) were significantly ($p = .042$) lower than normal control ($1.01 \pm 0.04 \times 10^{-3}$ mm^2/s). Fig. 1 shows a representative example of a boy with Leigh's disease and dysmyelination in the medulla-cervical cord, bilateral substantia nigra, colliculi, periaqueductal gray matter and occipital periventricular white matter.

There were six children with chromosomal abnormalities including chromosome 8 duplication, chromosome 12 inversion, chromosome 1q deletion and 3q duplication, proximal 15q deletion, partial deletion of chromosome 18, and mosaic XX and XY. Conventional MRI demonstrated structural abnormality of the brain in these children including microencephaly (5), agenesis of corpus callosum (3), hydrocephalus (2), lissencephaly (1), and delayed myelination (1). ADCs of substantia nigra ($1.09 \pm 0.10 \times 10^{-3}$ mm^2/s) were significantly ($p = .046$) higher than normal control ($1.01 \pm 0.05 \times 10^{-3}$ mm^2/s).

Of seven children with genetic syndromes, MRI was normal on a child with type 7 glycogen storage disease. The remaining six children with X-linked congenital hydrocephalus (2), metabolic myopathy with myoadenylate deaminase deficiency, Prune Belly syndrome, Cono Renal syndrome, and Pierre Robin syndrome had brain malformation including T2 prolongation in the white matter and deep gray nuclei (3), agenesis of corpus callosum (2), aqueduct stenosis (2), lissencephaly (2), and microencephaly (2). MTRs of globus pallidus ($44.81 \pm 1.56\%$) were significantly ($p = .018$) higher than normal control ($41.87 \pm 0.70\%$).

Conventional MRI depicted T2 prolongation in the white matter, lacunar infarct in the putamen or hypoplastic corpus callosum in three of five children with previous viral encephalitis. The mean ADCs of cortical gray matter ($1.22 \pm 0.29 \times 10^{-3}$ mm^2/s) were significantly ($p = .043$) higher than normal control ($1.03 \pm 0.12 \times 10^{-3}$ mm^2/s).

In two children with vitamin B12 deficiency, conventional MRI showed brain atrophy. There was no significant difference in the MTRs and ADCs of all brain structures compared to normal control.

In 13 children with clinical suspicion of cerebral palsy, conventional MRI depicted T2 prolongation in the white matter (5), polymicrogyria (2), and hypogenesis of corpus callosum (1). The ADCs of tectum ($1.10 \pm 0.11 \times 10^{-3}$ mm^2/s) were significantly ($p = .023$) lower than normal control ($1.18 \pm 0.08 \times 10^{-3}$ mm^2/s).

Conventional MRI was normal in all 19 children without an identified cause for GDD. There was also no significant difference in the MTRs and ADCs of all brain structures compared to normal control.

4. Discussion

Conventional MRI, T2 measurement, ADC and MTR determination have been used to study the white matter maturation in normal children and to assess various developmental, metabolic and neurodegenerative disorders [24–28]. At birth there is a reverse adult pattern with low T1 and high T2 signal intensities in the white matter and deep gray nuclei. Highest MTR and shortest T2 are found in posterior pons, mesencephalon and middle cerebellar peduncle, lowest MTR and longest T2 in frontal and occipital white matter. Myelination has occurred in the pons, posterior limb of internal capsule and cerebellar peduncle at birth, optic radiation and splenium before 3 months, anterior limb of internal capsule and genu before 6 months, white matter of frontal, parietal and occipital lobes before12 months of age [24]. Cholesterol, phospholipids, sphingomyelin, cerebroside and sulfatides increase with active myelin synthesis whereas the total water content of brain decreases from 90% at birth to 82% in childhood. MTR depends on concentration of macromolecules, surface chemistry and biophysical dynamics of macromolecules. Myelin, cerebrosides and phospholipids contribute to increased MTR during myelination with concomitant decrease in ADC. The inverse relationship between MTR and ADC reflects a shift from mobile to immobile tissue protein. After complete myelination, the corpus callosum has only myelinated white matter and highest MTR; mesencephalon and anterior pons have lowest MTR [25–27]. In our study, conventional MRI demonstrated abnormal brain anatomy or T2 prolongation in all of the 41 children with congenital brain malformation, metabolic and chromosomal disorders, and vitamin B12 deficiency. Of the seven children with genetic syndrome, 85.71% were also shown to have brain malformation. Conventional MRI demonstrated encephalomalacia in 60% of the five children with history of viral encephalitis. Eight of the 13 children with clinical suspicion of cerebral palsy had abnormal MRI findings that may help to reclassify them as having congenital malformation. All 19 children who were eventually classified as idiopathic GDD had normal MRI. The diagnostic yield of electroencephalogram, metabolic screening, cytogenetic testing and skin/muscle biopsy was low at 62.50, 24.71, 22.22, and 19.05%, respectively. Although the findings of abnormal myelination or brain

anatomy were non-specific, conventional MRI was a useful adjunct to detailed history and physical examination in the decision-making concerning further metabolic and cytogenetic testing, and muscle biopsy.

Other investigators have reported zones of increased diffusion in the white matter and deep gray nuclei of children with leukodystrophy, metabolic disorders and neurodegenerative disorders. The increased diffusion has been attributed to impaired myelination or demyelination with myelin splitting and vacuolization [11,27–33]. Low ADCs have been found in pyramidal tracts and dentate nuclei of infantile neuroaxonal dystrophy reflecting dystrophic axons with restricted mobility of water molecules [34]. Demyelination is associated with decreased MTR whereas high MTR is seen in wallerian degeneration because of axonal collapse, destruction of myelin, removal of myelin, fibrosis and atrophy [11,30]. We observed lower MTRs in the cortical gray matter but higher MTRs in the thalamus and lower ADCs in the tectum of children with brain malformation. There were higher ADCs in the parietal white matter, higher MTRs in the putamen and lower ADCs in the substantia nigra of children with metabolic disorders. We also found elevation of ADCs in the substantia nigra of children with chromosomal abnormality, increased MTRs in the globi pallidi of children with genetic syndromes, and higher ADCs in the cortical gray matter of children with previous viral encephalitis. These abnormal ADCs and MTRs may result from different degrees of dysmyelination, myelin destruction and fibrosis. There was no specific pattern of ADC and MTR alteration to aid the differential diagnosis of GDD in these children. The lower ADCs in the tectum of children with cerebral palsy and the abnormal findings of T2 prolongation in the white matter, polymicrogyria and hypoplastic corpus callosum in 8/13 children on conventional MRI suggest that some of these children may be re-classified as having brain malformation.

Our study was limited by the small sample size in each category of GDD. The control group consisted of children who had normal developmental milestones prior to the diagnosis of brain tumors. Another limitation of this study was the use of manual placement of ROI on various parts of the brain for determination of MTR and ADC. Semi-automatic computer segmentation technique to isolate these structures may allow a more accurate analysis [35]. Further study using healthy children with normal neuropsychological testing as normal control and larger sample size of different causes of GDD is necessary to determine any specific pattern of MTR and ADC changes in GDD.

5. Summary

Conventional MRI complements detailed history and physical examination in the decision-making concerning further metabolic and cytogenetic testing, and muscle biopsy in children with GDD. We did not find a specific pattern of ADC and MTR alteration to aid the differential diagnosis of GDD.

References

[1] Yeargin-Allsopp M, Murphy CC, Cordero JF. Reported biochemical causes and associated medical conditions for mental retardation among 10 year old children, metropolitan Atlanta, 1985 to 1987. Dev Med Child Neurol 1997;39: 142–9.

[2] Schouman-Claeys E, Picard A, Lalande G, Kalifa G, Lacert P, Brentanos E, et al. Contribution of computed tomography in the aetiology and prognosis of cerebral palsy in children. Br J Radiol 1989;62:248–52.

[3] Kolawole TM, Patel PJ, Mahdi AH. Computed tomographic (CT) scans in cerebral palsy (CP). Pediatr Radiol 1989;20:23–7.

[4] Demaerel P, Kingsley DP, Kendall BE. Isolated neurodevelopmental delay in childhood: clinicoradiological correlation in 170 patients. Pediatr Radiol 1993;23:29–33.

[5] Curry CJ, Stevenson RE, Aughton D, Byrne J, Carey JC, Cassidy S, et al. Evaluation of mental retardation: recommendations of a consensus conference: American College of Medical Genetics. Am J Med Genet 1999;82:60–6.

[6] Shevell MI, Majnemer A, Rosenbaum P, Abrahamowicz M. Etiologic yield of subspecialists' evaluation of young children with global developmental delay. J Pediatr 2000;136:593–8.

[7] Majnemer A, Shevell MI. Diagnostic yield of the neurologic assessment of the developmentally delayed child. J Pediatr 1995; 127:193–9.

[8] Battaglia A, Bianchini E, Carey JC. Diagnostic yield of the comprehensive assessment of developmental delay/mental retardation in an institute of child neuropsychiatry. Am J Med Genet 1999;82: 60–6.

[9] Shevell M, Ashwal S, Donley D, Flint J, Gingold M, Hirtz D, et al. Practice parameter: evaluation of the child with global developmental delay. Report of the Quality Standards Subcommittee of the American Academy of Neurology and the Practice Committee of the Child Neurology Society. Neurology 2003;60:367–80.

[10] Burke JW, Mathews VP, Elste AD, Ulmer JL, McLean FM, Davis SB. Contrast-enhanced magnetization transfer saturation imaging improves MR detection of herpes simplex encephalitis. Am J Neuroradiol 1996;17:773–6.

[11] Melhem ER, Breiter SN, Ulug AM, Raymond GV, Moser HW. Improved tissue characterization in adrenoleukodystrophy using magnetization transfer imaging. Am J Roentgenol 1996;166:689–95.

[12] Inglese M, Salvi F, Iannucci G, Mancardi GL, Mascalchi M, Filippi M. Magnetization transfer and diffusion tensor MR imaging of acute disseminated encephalomyelitis. Am J Neuroradiol 2002;23: 267–72.

[13] Prager JM, Rosenblum JD, Huddle DC, Diamond CK, Metz CE. The magnetization transfer effect in cerebral infarction. Am J Neuroradiol 1994;15:1497–500.

[14] Okumura A, Takenaka K, Nishimura Y, Asano Y, Sakai N, Kuwata K, et al. The characterization of human brain tumor using magnetization transfer technique in magnetic resonance imaging. Neurol Res 1999; 21:250–4.

[15] Boorstein JM, Wong KT, Grossman RI, Bolinger L, McGowan JC. Metastatic lesions of the brain: imaging with magnetization transfer. Radiology 1994;191:799–803.

[16] Kabani NJ, Sled JG, Shuper A, Chertkow H. Regional magnetization transfer ratio changes in mild cognitive impairment. Magn Reson Med 2002;47:143–8.
[17] Pen SSF, Tseng WYI, Liu HM, Li YW, Huang KM. Diffusion-weighted images in children with meningoencephalitis. Clin Imaging 2003;27:5–10.
[18] Tsuchiya K, Katase S, Yoshino A, Hachiya J. MRI of influenza encephalopathy in children: value of diffusion-weighted imaging. J Comput Assist Tomogr 2000;24:303–7.
[19] Cowan FM, Pennock JM, Hanrahan JD, Manji KP, Edwards AD. Early detection of cerebral infarction and hypoxic ischemic encephalopathy in neonates using diffusion-weighted magnetic resonance imaging. Neuropediatrics 1994;25:172–5.
[20] Robertson RL, Maier SE, Robson CD, Mulkern RV, Karas PM, Barnes PD. MR line scan diffusion imaging of the brain in children. Am J Neuroradiol 1999;20:419–25.
[21] Tzika AA, Zarifi MK, Goumnerova L, Astrakas LG, Zurakowski D, Young-Poussaint T, et al. Neuroimaging in pediatric brain tumors: Gd-DTPA-enhanced, hemodynamic, and diffusion MR imaging compared with MR spectroscopic imaging. Am J Neuroradiol 2002; 23:322–33.
[22] Pui MH. Magnetization transfer analysis of brain tumor, infection, and infarction. J Magn Reson Imaging 2000;12:395–9.
[23] Pui MH, Wang YD. Magnetization transfer and diffusion MRI of brain tumor, infection and infarct in children. Clin Imaging 2005;29:162–71.
[24] Paus T, Collins DL, Evans AC, Leonard G, Pikem B, Zijdenbos A. Maturation of white matter in the human brain: a review of magnetic resonance studies. Brain Res Bull 2001;54:255–66.
[25] Toft PB, Leth H, Peitersen B, Lou HC, Thomsen C. The apparent diffusion coefficient of water in grey and white matter of the infant brain. J Comput Assist Tomogr 1996;20:1006–11.
[26] Morriss MC, Zimmerman RA, Bilaniuk LT, Hunter JV, Haselgrove JC. Changes in brain water diffusion during childhood. Neuroradiology 1999;41:929–34.
[27] Engelbrecht V, Rassek M, Preiss S, Wald C, Modder U. Age-dependent changes in magnetization transfer contrast of white matter in the pediatric brain. Am J Neuroradiol 1998;19:1923–9.
[28] Rossi A, Biancheri R, Bruno C, Rocco MD, Calvi A, Pessagno A, et al. Leigh Syndrome with COX deficiency and SURFI gene mutations: MR imaging findings. Am J Neuroradiol 2003;24: 1188–91.
[29] Gelal FM, Grant PE, Fischbein NJ, Henry RG, Vigneron DB, Barkovich AJ. The role of isotropic diffusion MRI in children under 2 years of age. Eur Radiol 2001;11:1006–14.
[30] Engelbrecht V, Rassek M, Gärtner J, Kahn T, Mödder U. The value of new MRI techniques in adrenoleukodystrophy. Pediatr Radiol 1997; 27:207–15.
[31] Sener RN. Metachromatic leukodystrophy: diffusion MR imaging findings. Am J Neuroradiol 2002;23:1424–6.
[32] Sener RN. L-2 hydroxyglutaric aciduria: proton magnetic resonance spectroscopy and diffusion magnetic resonance imaging findings. J Comput Assist Tomogr 2003;27:38–43.
[33] Sener RN. Canavan disease: diffusion magnetic resonance imaging findings. J Comput Assist Tomogr 2003;27:30–3.
[34] Sener RN. Diffusion magnetic resonance imaging in infantile neuroaxonal dystrophy. J Comput Assist Tomogr 2003;27:34–7.
[35] Raff U, Rojas GM, Huete I, Hutchinson M. Computer assessment of neurodegeneration in Parkinson disease using data fusion techniques with MR images. Acad Radiol 2003;10:1036–44.

Dr Margaret Pui is an associate professor in Radiology at McMaster University. Her subspecialties include MRI and Nuclear Medicine. She has worked in Canada, USA, Singapore, China, Pakistan, and Bermuda. Her visiting professorship includes various universities in China and South Africa.

Dr Yongdong Wang was a research fellow in Radiology at McMaster University. He has special interest in MRI and breast imaging. He is now professor of Radiology at Taishan Medical College in Shandong, China.

Dr Nina Singh was an MRI fellow and is now assistant professor in Radiology at McMaster University.